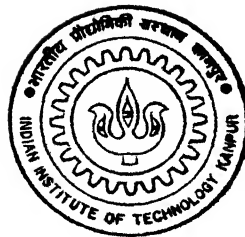


WALL BOUNDARY CONDITIONS FOR INVISCID COMPRESSIBLE FLOWS

by
NARENDRABABU. B.



ME
1997
M
NAR
WAL

DEPARTMENT OF MECHANICAL ENGINEERING
INDIAN INSTITUTE OF TECHNOLOGY KANPUR
May, 1997

WALL BOUNDARY CONDITIONS FOR INVISCID COMPRESSIBLE FLOWS

A Thesis Submitted
in Partial Fulfillment of the Requirements
for the Degree of

MASTER OF TECHNOLOGY

by

NARENDRABABU .B.

to the

**DEPARTMENT OF MECHANICAL ENGINEERING
INDIAN INSTITUTE OF TECHNOLOGY KANPUR**

May, 1997

3 - JUN 1997/ME

CENTRAL LIBRARY
I. I. T., KANPUR

No. A123490

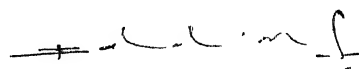
ME-1997-M-NAR-WAL

CERTIFICATE

It is certified that the work contained in the thesis entitled "*Wall Boundary Conditions for Inviscid Compressible Flows*", by *Narendrababu .B.*, has been carried out under our supervision and that this work has not been submitted elsewhere for a degree.

(On leave)
Gautam Biswas
Professor

Department of Mechanical Engineering
I.I.T., Kanpur



N. Balakrishnan
Visiting Faculty

Department of Mechanical Engineering
I.I.T., Kanpur

May, 1997.

Dedicated
to
my Parents

Acknowledgements

I express my thanks to Dr.N.Balakrishnan and Dr.Gautam Biswas for their guidance and support I received throughout my Thesis work. I am grateful to their friendly and encouraging nature. I owe the greatest debt to them.

I am deeply indebted to all my CFD Labmates for their suggestions and cooperation. My thanks are also due to my classmates and friends for making my stay at IIT Kanpur a memorable one.

I am specially thankful to my kannada friends for thier support and cooperation all the time. I would like to remember my assosiation with the kannada sangha and its festivals.

Abstract

Solving the Euler Equations numerically is one of the central issues of the CFD community. Accuracy of these solutions not only depend on the scheme used, but also strongly depend on the Wall Boundary treatment. We discuss both the Strong Formulation where the zero normal velocity on the Wall is enforced explicitly and the Weak Formulation where the zero normal velocity on the Wall is enforced through the Flux function. Taking into account the advantages of both these Boundary Conditions, Mixed Wall Boundary Conditions have been proposed. We discuss here, the Merits and Demerits of the Mixed Wall Boundary Conditions with respect to the Mirror Wall Boundary Conditions which is a Weak Formulation. Numerical Comparison between the Mixed and Mirror Wall Boundary Conditions for the Subsonic and Transonic cases has been made for the Airfoil NACA0012 with the van Leer and Roe Schemes. The Comparison between the two Boundary Conditions has also been made for the Supersonic flow through an Expansion Channel. These Comparisons point out that the Mixed Wall Boundary Conditions are less dissipative than the Mirror Wall Boundary Conditions.

Contents

List of Figures	viii
List of Tables	x
Nomenclature	xi
1 Introduction	1
1.1 Introduction	1
1.2 Classification	2
1.3 Literature Survey	3
2 Formulation and Flux formulae	7
2.1 2-D Euler equations	7
2.2 Finite Volume Schemes	8
2.2.1 Higher Order Finite Volume Schemes	9
2.2.2 Cell calculations	10
2.2.3 Method of Least Squares	11
2.3 Flux Calculation	13
2.3.1 Hyperbolicity of Euler equations	13

2.3.2	Flux Vector Splitting Schemes	15
2.3.3	Flux Difference Splitting(FDS)	17
2.4	Summary	19
3	Wall Boundary Conditions	20
3.1	Strong formulation	22
3.2	Weak formulation	25
3.2.1	Mirror condition	25
3.3	Mixed Boundary Condition	27
3.4	Summary	28
4	Results and Discussions	29
4.1	Subsonic flow past NACA 0012	30
4.2	Transonic flow past NACA 0012	32
4.3	Supersonic Flow Through an Expansion Channel	33
	Bibliography	49

List of Figures

2.1	Control volume Ω_i	8
2.2	A typical two dimensional finite volume cell.	11
2.3	A typical 2-D Finite volume Cell and its neighbours.	12
2.4	Flux vector splitting	16
3.1	Directions of information flow at the Wall boundary	21
3.2	Mirror boundary condition	26
4.1	Grids used	34
4.2	MACH CONTOURS WITH VAN LEER SCHEME (Mach No. = 0.63 and Alpha = 2.00 degrees)	35
4.3	WALL ENTROPY FOR THE VAN LEER SCHEME (Mach No = 0.63 and Alpha = 2.00 degrees)	36
4.4	MACH CONTOURS WITH ROE-LEER SCHEME (Mach No. = 0.63 and Alpha = 2.00 degrees)	37
4.5	WALL ENTROPY FOR THE ROE-LEER SCHEME (Mach No = 0.63 and Alpha = 2.00 degrees)	38
4.6	MIXTURE OF MIRROR AND MIXED BOUNDARY CONDI- TION	39
4.7	MACH CONTOURS WITH LEER SCHEME (Mach No. = 0.8 and Alpha = 1.25 degrees)	40

4.8	WALL ENTROPY FOR THE LEER SCHEME (Mach No = 0.8 and Alpha = 1.25 degrees)	41
4.9	MACH CONTOURS WITH ROE-LEER SCHEME (Mach No. = 0.8 and Alpha = 1.25 degrees)	42
4.10	WALL ENTROPY FOR THE ROE-LEER SCHEME (Mach No = 0.8 and Alpha = 1.25 degrees)	43
4.11	MACH CONTOURS WITH VAN LEER SCHEME (Mach No. = 2.0)	44
4.12	WALL ENTROPY COMPARISON	45

List of Tables

4.1 Grid details 30

Nomenclature

A	Flux Jacobian $\left(\frac{\partial F}{\partial U}\right)$
a	Sonic Speed $\left(\sqrt{\frac{\gamma p}{\rho}}\right)$
e	Total Energy per unit volume
F	Flux vector
L	Left eigenvectors of the flux Jacobian A
M	Mach number
\hat{n}	unit vector normal to the cell interface
p	Pressure
R	Matrix of the right eigenvectors of the flux Jacobian A
\vec{r}	Right eigenvector of the flux Jacobian A
t	Time
U	Vector of Conserved variables
u	Fluid velocity in x direction
u_{\perp}	Fluid normal velocity to the cell interface
V	Vector of primitive variables
v	Fluid velocity in y direction
w	Fluid velocity in z direction
x,y,z	Coordinates
γ	Ratio of specific gases
Λ	Diagonal Matrix with eigenvalues of A as the entries along the diagonal
λ	Eigenvalue of the flux Jacobian A
ϕ	Dissipation control parameter
ρ	Density

Superscripts

+ Corresponding to the positive part of the flux vector

- Corresponding to the negative part of the flux vector

Subscripts

- k Represents the k^{th} cell
L Refers to the state to the left of the cell interface
R Refers to the state to the right of the cell interface

Chapter 1

Introduction

1.1 Introduction

The Engineering fluid dynamic problems of the eighteenth, nineteenth and early twentieth centuries almost always involved either the flow of liquids or the low speed flow of gases ;for both the cases the assumption of constant density is quite valid. However, with the advent of high speed flows, exemplified by the de Laval's convergent - divergent nozzle design and the supersonic sonic flight of the Bell Xs-1, the density can no longer be assumed constant throughout the flow field. Indeed, for such flows the density can sometimes vary by orders of magnitude. In this light, we deal here with compressible flows, in which the density is not constant.

The mathematical description of fluid motion in the form of PDE's by Euler not only enriched the science of mathematics but also was responsible for the development of a number of useful analytical tools in theoretical fluid dynamics as solutions to these PDE's. A finer mathematical description of the fluid, wherein the viscous effects are included was given by Navier and Stokes in the nineteenth century. From there on the fluid dynamicists have been relentlessly attempting to obtain the closed form solutions to these equations.

Computational Fluid Dynamics(CFD) means solving numerically, Euler and Navier-Stokes equations either in their original form or approximate form on a discretised space or time domain. With the advent of high speed computers, CFD has gained the credibility as a reliable design tool in the latter half of this century. Many numerical schemes have been proposed to solve the Euler equations. The schemes of Lax and Wendroff [2], Mac Cormack [3] and Jameson [4] are some of the well known schemes, which are purely mathematical in nature, where as Upwind schemes are based on physics of the fluid flow. There are two categories of Upwinding schemes such as Finite Vector Splitting(FVS) and Finite Difference Splitting(FDS) schemes. The principle of FVS is to split flux vector into a positive and negative parts such that the positive flux Jacobian has all the positive eigenvalues and the negative flux Jacobian has all the negative eigenvalues. The FDS schemes are based on the classical initial value problem called Riemann problem. The accuracy of the solutions thus obtained not only depend on the accuracy of the scheme, but also strongly depend on the Wall boundary treatment. The solution accuracy and stability very strongly depend on the boundary procedures adopted in enforcing the wall boundary conditions. So, proper treatment of the wall boundary conditions is essential for obtaining reliable results. Therefore, we have tried to look into this aspect here.

1.2 Classification

Accurate satisfaction of the boundary conditions is one of the central issues in any CFD problem. A solution acquires a special flavor because of the boundary conditions of the problem. One way of classifying the boundary conditions is (a).Physical boundary conditions such as flow tangency, no-slip, pressure on the exit plane etc. (b). Fictitious boundary conditions which are usually required at the farfield boundary of a finite sized computational domain. In the

language of Moretti such farfield boundary conditions are *mathematical model for the rest of the universe*. van Leer calls (a) type Boundary Conditions as *real* Boundary Conditions and (b) type Boundary Conditions as *artificial* Boundary Conditions. There is one more way of classifying Boundary Conditions. (a) Dirichlet Boundary Condition. (b) Neumann Boundary Condition. If the Boundary Conditions are directly specified on the unknowns u and v , then such Boundary Conditions are Dirichlet Boundary Conditions, where as if the Boundary Conditions are specified on the derivatives of the unknowns, such type are called Neumann type of Boundary Conditions. For example, no-slip condition for viscous flows is a Dirichlet Boundary Condition while, the flow tangency condition in terms of the full potential is a Neumann type Boundary Condition.

1.3 Literature Survey

Two basically different approaches can be found in the literature to introduce Wall Boundary Conditions for the Euler equations. In one approach, the unknown along the boundary are determined from inside the domain by some space extrapolation technique under the constraint that the unknowns must satisfy the Boundary Conditions. Various methods have been proposed. The use of normal momentum equation for pressure extrapolation at a solid wall belongs to this approach.

A second approach follows more closely the physics of the hyperbolic equations by discretising the compatibility equations for the outgoing characteristic variables, while replacing the ingoing characteristic information by the physical Boundary Conditions. Consistent Boundary Conditions for the cell centered upwind finite volume Euler solvers proposed by Deconinck and Struys [5] belongs to this second approach. In this approach, from the consistency

condition for a numerical flux function, the unknowns along the boundary are determined such that the numerical flux function based on the boundary and adjacent interior variables leads to a flux which satisfies the Boundary Condition. This boundary treatment reduces to characteristic boundary conditions for the case of a linear hyperbolic systems of equations.

Direction of information propagation at the boundaries must be properly taken care. As Butler [7], points that use of a special scheme at the boundary, violates the global conservation, causes inconsistency, and many lead to artificial boundary layer of numerical error. Instead he proposes to evaluate boundary points by relating them to interior values by the theory of characteristics. This approach has been used for treating conditions at both shock-wave and solid boundary [8]. An alternative to the theory of characteristics at a solid body is to use the knowledge that a streamline in two dimensions and a stream surface in a three dimensions wet the surface of a body in inviscid flow. This information, when coupled with the solid wall boundary condition and incorporated into the momentum equation, which leads to relation that connects boundary points to those in the interior. For sometime various workers used this so-called normal momentum equation but usually for only simple body shapes and coordinate systems. Mac Cormack [9], presented a general expression valid for any geometry, but one that requires labourious interpolation between grid points. Later on Rizzy [10], gave an equally general formulation that avoided the need for interpolation. Followed by that, Rizzy [11], presented the derivation for his auxiliary equation and demonstrated how it is computationally more convenient to apply because it requires no interpolation of computed flow properties, but rather uses data only at the grid points, a particular advantage in three dimensions.

One of the common procedures found in the literature is the Mirror condition in which the approximate Riemann solver used for determining fluxes in the interior edges is used on the wall boundary also. For this, a fictitious state

is determined in such a way that the zero normal mass flux across the wall is guaranteed. So, based on the information obtained from interior and fictitious states, the fluxes on the wall are calculated in a way similar to that used in the interior. Its main advantage is that it takes into account, the direction of propagation of information. It also converges fast. Its main disadvantage is the numerical dissipation that it produces. Moretti [12] is a strong critic of this method. While criticising this method he says that many authors use what they call a *reflection principle* which is not a principle at all and should rather be called a reflection technique. He also points out that there is no precise definition for such a technique in the literature. All the Physical parameters are specularly reflected on the rigid wall except the normal velocity which is assumed as antisymmetric. These assumptions force the normal derivatives of these variables to vanish at the wall. Here, the assumption $\frac{\partial p}{\partial n} = 0$ does not take into account the curvature effects. Hence, he argues that even some of the assumptions made in this procedure are physically wrong.

Various approaches can be found in the literature to introduce wall Boundary Conditions for the Euler equations. But, all these schemes one way or the other way boils down to the enforcement of zero normal velocity on the solid wall boundary. Based on the method of enforcement of zero normal velocity on the solid wall, these formulations can be classified into strong and weak formulations. In the strong formulation, the zero normal velocity on the wall is enforced explicitly, whereas in weak formulation, the zero normal velocity is enforced through the flux function. Taking into advantage of both the approaches Mixed boundary procedures have been developed [1].

Improper treatment of wall boundary conditions allow numerical dissipation to creep into the solution. So, the Wall Boundary Conditions play an important role in obtaining the proper results. The Strong Formulation which we discuss later, violates the global conservation whereas, the Weak Formulation such as Mirror Wall Boundary Condition does not take into account the cur-

vature effects and are less dissipative. The Mixed Boundary Condition which has the advantages of both these Schemes is expected to be less dissipative. Since, the numerical dissipation can spoil any solution, it becomes important to keep this in check. It is in this context that we are looking at the Mirror and the Mixed Wall Boundary Conditions which are discussed in the subsequent chapters. In our work, we have applied the above stated Mixed boundary procedure to cell centered finite volume schemes on structured meshes. Here, we have tried to examine the problem of numerical dissipation in Mixed and Mirror wall boundary conditions.

Chapter 2

Formulation and Flux formulae

2.1 2-D Euler equations

The 2-D Euler equations of Gas Dynamics can be written in the differential form of conservation law as,

$$\frac{\partial U}{\partial t} + \frac{\partial F}{\partial x} + \frac{\partial G}{\partial y} = 0 \quad (2.1)$$

where, U is the vector of conserved variables and F and G are flux vectors in the x and y directions respectively. They are defined by the relations:

$$U = \begin{bmatrix} \rho \\ \rho u \\ \rho v \\ e \end{bmatrix}; F = \begin{bmatrix} \rho u \\ \rho u^2 + p \\ \rho uv \\ (e + p)u \end{bmatrix}; G = \begin{bmatrix} \rho v \\ \rho uv \\ \rho v^2 + p \\ (e + p)v \end{bmatrix} \quad (2.2)$$

where, ρ is the mass density, u is the x -component of the velocity vector, v is the y -component of velocity vector, p is the pressure and e is the total energy per unit volume given by,

$$e = \frac{p}{\gamma - 1} + \frac{\rho(u_{\parallel}^2 + u_{\perp}^2)}{2} \quad (2.3)$$

2.2 Finite Volume Schemes

Using the Gauss theorem the state update formula for finite volume is written as

$$\left(\frac{\partial U_i}{\partial t} \right) = -\frac{1}{\Omega_i} \oint_{\partial\Omega_i} F_{\perp}(U(\vec{r}, t)) ds \quad (2.4)$$

where, the vector of state variables $U = (\rho, \rho\vec{u}, E)^T$ represent the mass density, momentum components and total energy per unit volume. The subscript i represents the i^{th} finite volume Ω_i . The Euler flux normal to the finite volume interface $\partial\Omega_i$ is given by

$$F_{\perp} = F \cdot \hat{n} = (\rho u_{\perp}, \rho u_{\perp} \vec{u} + p \hat{n}, (E + p) u_{\perp})^T \quad (2.5)$$

where, \hat{n} is the outward unit normal, $u_{\perp} = \vec{u} \cdot \hat{n}$ and $u_{\parallel} = \vec{u} \wedge \hat{n}$ are the normal and tangential velocities respectively. The pressure p is given by

$$p = (\gamma - 1) \left(E - \frac{1}{2} \rho (u_{\perp}^2 + u_{\parallel}^2) \right) \quad (2.6)$$

where, $\gamma = 1.4$ is the specific heat ratio.

It is possible to build finite volume schemes either in cell vertex or cell center framework. Typical cell vertex and cell center finite volumes on a quadrilateral domain are shown in fig.2.1:

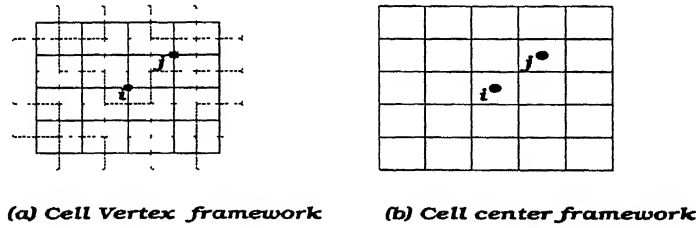


Figure 2.1: Control volume Ω_i

In cell vertex finite volume framework, the state variables are updated at the nodes whereas, in cell center finite volume framework, the state variables

are updated at the centroids of the cells. We shall refer to these points as *reference points*.

In the case of cell center finite volume schemes, as the *reference points* lie at the center of the cell, they do not lie on the boundaries. Whereas, in the case of the cell vertex finite volume schemes, as the *reference points* are the nodes of the cells, they lie on the boundaries. So, there will be difference in the way the boundary conditions are implemented in these two schemes. In cell vertex finite volume schemes, the boundary conditions are enforced explicitly on the *reference points* whereas, in the cell center finite volume schemes, the boundary conditions are enforced through the flux function. As we have used the cell center finite volume schemes, we have applied the latter method.

2.2.1 Higher Order Finite Volume Schemes

For steady state computations, the accurate calculation of fluxes on the cell interface using higher order spatial accurate schemes is very important. The time integration can be done by using either implicit schemes or multistage schemes. For achieving high order spatial accuracy on structured meshes, we are made using the MUSCL (monotonic upstream centered schemes for conservation laws.) (Anderson, et.al [13]) extrapolation. The conserved variables are extrapolated on to the cell interfaces for subsonic and supersonic cases and for hypersonic cases, the primitive variables (as done by Sreekanth and Reddy [1992a] are extrapolated. The one parameter family of schemes called κ - schemes are used in MUSCL extrapolation are given below :

$$\left. \begin{aligned} W_L &= W_k + \frac{\phi k}{4} ((1 - \kappa)(W_k - W_{k-1}) + (1 + \kappa)(W_{k+1} - W_k)) \\ W_R &= W_k - \frac{\phi k}{4} ((1 + \kappa)(W_{k+1} - W_k) + (1 - \kappa)(W_{k+2} - W_{k+1})) \end{aligned} \right\} \quad (2.7)$$

where W represents either the conserved variable U or the primitive variable V , as the case may be. For $\phi = 0$ we obtain a first order scheme. For $\phi = 1$

where W represents either the conserved variable U or the primitive variable V , as the case may be. For $\phi = 0$ we obtain a first order scheme. For $\phi = 1$ we have the following schemes for different values of κ : $\kappa = -1$ (second order - Upwind), $\kappa = 1$ (second order - Central), $\kappa = 0$ (Fromm Scheme), $\kappa = \frac{1}{2}$ (QUICK), $\kappa = \frac{1}{3}$ (Third Order - Upwind Biased). The spurious oscillations that appear in the solution because of use of high resolution schemes can be suppressed using van Albada limiter (Anderson, et.al [13]):

$$\phi_k = \frac{2\Delta_+ W_k \Delta_- W_k + \epsilon}{\Delta_+ W_k^2 + \Delta_- W_k^2 + \epsilon} \quad (2.8)$$

where,

$$\left. \begin{aligned} \Delta_+ W_k &= W_{k+1} - W_k \\ \Delta_- W_k &= W_k - W_{k-1} \end{aligned} \right\} \quad (2.9)$$

Here ϵ is a small number added to avoid fault of divide fault during the computation. In all the higher order computations on structured mesh presented in this thesis κ is chosen to be $\frac{1}{3}$.

2.2.2 Cell calculations

The space discretised finite volume form of the Euler equations is given by,

$$\left(\frac{\partial U_k}{\partial t} \right)^n = - \frac{1}{V_k} \sum_m F_{\perp}^m \Delta s^m \quad (2.10)$$

where the subscript k denotes the cell number, m is the edge index (or interface index) of the k^{th} cell and the subscript n denotes the time step. F^m and Δs^m are respectively the normal flux and the area of the m^{th} face. Further, V_k is the volume of the k^{th} cell. The vector of conserved variable U and the flux vector F^m are given by,

$$U = \begin{bmatrix} \rho \\ \rho u \\ \rho v \\ e \end{bmatrix}; F_{\perp}^m = \begin{bmatrix} \rho u_{\perp} \\ \rho u u_{\perp} + p n_x \\ \rho v u_{\perp} + p n_y \\ (e + p) u_{\perp} \end{bmatrix} \quad (2.11)$$

Where, n_x and n_y represent the direction cosines of the unit normal \hat{n} to the interface and are given by,

$$n_x = \frac{\Delta y}{\Delta s}, n_y = -\frac{\Delta x}{\Delta s} \quad (2.12)$$

It is very essential to know about the cell and its related data for the under-

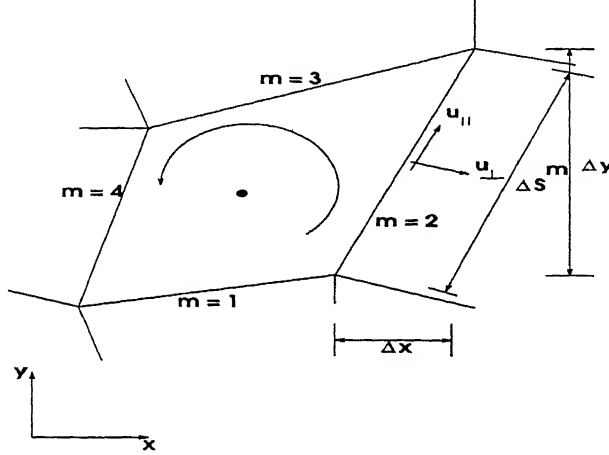


Figure 2.2: A typical two dimensional finite volume cell.

standing of any numerical code. So we are presenting a typical finite volume cell and the way fluxes are calculated on each edge of the cell as shown in the fig 2.2.

2.2.3 Method of Least Squares

The gradient terms in this work are obtained using the method of least squares. Here the gradient terms are obtained by minimising sum of the squares of the errors [14], defined by

$$E_i = \sum_{j=1}^N (\Delta\phi_i - (\nabla\phi)_i \cdot \Delta\vec{r}_j)^2 \quad (2.13)$$

where, subscript j represents the neighbouring grid points, N is the number of support points, ϕ_i is the value obtained by the state update formula, $\Delta\phi_j =$

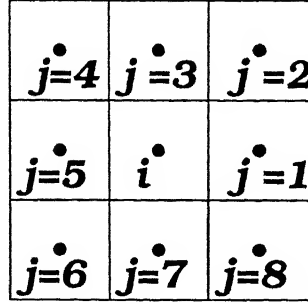


Figure 2.3 A typical 2-D Finite volume Cell and its neighbours.

$\phi_j - \phi_i$ and $\Delta \vec{r}_j = \vec{r}_j - \vec{r}_i$. We have considered all the neighbouring points ie $N = 8$ as shown in the fig2.3.

For a linear reconstruction procedure, it is possible to obtain a closed form expression for the gradient terms by minimising E_i which is defined above (eqn.no 2.13) and they are given by,

$$\phi_{i,x} = \frac{\| \Delta y \|^2 (\Delta x, \Delta \phi) - (\Delta x, \Delta y) (\Delta y, \Delta \phi)}{\| \Delta x \|^2 \| \Delta y \|^2 - (\Delta x, \Delta y)^2} \quad (2.14)$$

$$\phi_{i,y} = \frac{\| \Delta x \|^2 (\Delta y, \Delta \phi) - (\Delta x, \Delta y) (\Delta x, \Delta \phi)}{\| \Delta x \|^2 \| \Delta y \|^2 - (\Delta x, \Delta y)^2} \quad (2.15)$$

where,

$$\begin{aligned} \| \Delta x \|^2 &= \sum_{j=1}^N \Delta x_j^2, \quad (\Delta x, \Delta \phi) = \sum_{j=1}^N \Delta x_j \Delta \phi_j \\ \| \Delta y \|^2 &= \sum_{j=1}^N \Delta y_j^2, \quad (\Delta y, \Delta \phi) = \sum_{j=1}^N \Delta y_j \Delta \phi_j \end{aligned} \quad (2.16)$$

The above expressions (2.14) and (2.15) for the determination of the gradients of the variables are used in satisfying gradient boundary conditions on both structured and unstructured meshes. To calculate the Pressure at the Wall satisfying the normal momentum equation, the gradients of the conserved variables are required. these gradients are calculated using the above stated Least Square Formulae.

2.3 Flux Calculation

2.3.1 Hyperbolicity of Euler equations

One of the important features of the Hyperbolic conservation laws is that they have preferential direction of information propagation. This property is called as hyperbolicity property. This can be best understood by casting the Euler equations in the form of scalar convective equations. The 1D-Euler equations of Gas Dynamics can be written in the differential form of conservation laws as

$$\frac{\partial U}{\partial t} + \frac{\partial F}{\partial x} = 0 \quad (2.17)$$

where, U is the vector of conserved variables and F is the flux vector. They are defined by the relation

$$U = \begin{bmatrix} U_1 \\ U_2 \\ U_3 \end{bmatrix} = \begin{bmatrix} \rho \\ \rho u \\ e \end{bmatrix}; F = \begin{bmatrix} \rho u \\ \rho u^2 + p \\ (e + p)u \end{bmatrix} \quad (2.18)$$

Where, ρ is the mass density, u is the fluid velocity, p is the pressure and e is the total energy per unit volume given by,

$$e = \frac{p}{(\gamma - 1)} + \frac{\rho u^2}{2} \quad (2.19)$$

Eventhough F (2.18) is expressed as a function of primitive variables, ρ, u, p it can also be expressed in terms of the components of the vector of conserved variables U . We then obtain

$$F = \begin{bmatrix} U_2 \\ (\gamma - 1)U_3 + \frac{(3-\gamma)}{2} \frac{U_2^2}{U_1} \\ \gamma \frac{U_2 U_3}{U_1} - \frac{(\gamma-1)}{2} \frac{U_2^3}{U_1^2} \end{bmatrix} \quad (2.20)$$

Using the fact that $F = F(U)$ the equation(2.20) can be cast in the form of

$$\frac{\partial U}{\partial t} + A \frac{\partial U}{\partial x} = 0 \quad (2.21)$$

where the flux Jacobian matrix $A = \frac{\partial F}{\partial U}$ is given by

$$A = \begin{bmatrix} 0 & 1 & 0 \\ -\frac{(3-\gamma)}{2}u^2 & (3-\gamma)u & (\gamma-1) \\ -\frac{a^2 u}{(\gamma-1)} + \frac{(\gamma-2)}{2}u^3 & \frac{a^2}{(\gamma-1)} + \frac{(3-2\gamma)}{2}u^2 & \gamma u \end{bmatrix} \quad (2.22)$$

Here a is the sonic speed given by $a = \sqrt{(\gamma p)/\rho}$. The matrix A has all real eigen values and a complete set of linearly independent eigen vectors. Therefore the Euler equations are non-linear hyperbolic PDEs for the unknown U and must be solved with suitable boundary conditions. To cast Euler equations in the form of scalar convection equations, the flux Jacobian A is cast in the Jordan canonical form as follows:

$$A = R\Lambda L = R\Lambda R^{-1} \quad (2.23)$$

where, R and L are the matrices of right and left eigen vectors of A respectively and Λ is a diagonal matrix, the entries along the diagonal being the eigen values of A . The matrices R, Λ and L are given by:

$$R = \begin{bmatrix} 1 & 1 & 1 \\ u-a & u & u+a \\ \frac{u^2}{2} - ua + \frac{a^2}{(\gamma-1)} & \frac{u^2}{2} & \frac{u^2}{2} + ua + \frac{a^2}{(\gamma-1)} \end{bmatrix} \quad (2.24)$$

$$L = \begin{bmatrix} \frac{u}{2a} + \frac{(\gamma-1)}{4a^2}u^2 & -\frac{1}{2a} - \frac{(\gamma-1)}{2a^2}u & \frac{(\gamma-1)}{2a^2} \\ 1 - \frac{(\gamma-1)}{2a^2}u^2 & \frac{(\gamma-1)}{a^2}u & -\frac{(\gamma-1)}{a^2} \\ -\frac{u}{2a} + \frac{(\gamma-1)}{4a^2}u^2 & \frac{1}{2a} - \frac{(\gamma-1)}{2a^2}u & \frac{(\gamma-1)}{2a^2} \end{bmatrix} \quad (2.25)$$

$$\Lambda = \begin{bmatrix} u-a & 0 & 0 \\ 0 & u & 0 \\ 0 & 0 & u+a \end{bmatrix} \quad (2.26)$$

Therefore, substituting (2.20) into (2.18) gives

$$\frac{\partial U}{\partial t} + R\Lambda L \frac{\partial U}{\partial x} = 0 \quad (2.27)$$

Multiplying by L on both the sides, we get

$$L \frac{\partial U}{\partial t} + \Lambda L \frac{\partial U}{\partial x} = 0 \quad (2.28)$$

Letting $LdU = d\psi$, we get

$$\frac{\partial \psi}{\partial t} + \Lambda \frac{\partial \psi}{\partial x} = 0 \quad (2.29)$$

It should be noted that the convection equations defined above, are coupled through the dependence of λ_i and ψ_i on the components conserved variable vector U . Under the isentropic conditions, the ψ_i 's reduces to the well known riemann invariants. The hyperbolicity of Euler equations become more explicit and clearer from thier convective form of equations (eqn.no.2.29). The quantities ψ_i get convected with the speeds of the eigen values of the flux Jacobian A . Numerical schemes which follow the physics of the flow should take care of the propagation of information. The recent Upwind schemes such as Flux Vector Splitting and Flux difference Schemes take care of this hyperbolicity property of the Euler equations.

2.3.2 Flux Vector Splitting Schemes

Flux vector splitting is a technique for splitting the flux vector into *upwind components*. Here, the flux vector F is split into a positive part F^+ and a negative part F^- , such that the positive flux Jacobian has all the positive eigenvalues and the negative flux Jacobian has all the negative eigen values as follows :

$$F(U) = F^+(U) + F^-(U) \quad (2.30)$$

where , F^+ and F^- are are constructed such that

$$\frac{dF^+}{dU}(U) = A^+(U) \quad (2.31)$$

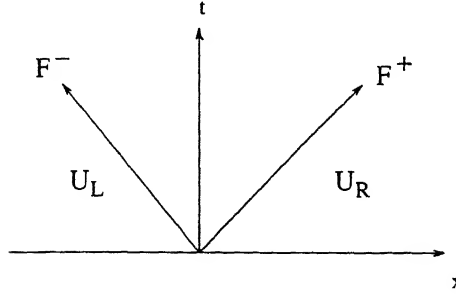


Figure 2.4: Flux vector splitting

$$\frac{dF^-}{dU}(U) = A^-(U)$$

The above equations imply that the eigenvalues of A^+ are nonnegative (≥ 0) and those of A^- are nonpositive (≤ 0). The numerical flux formula at an interface is given by

$$F(U_L, U_R) = F^+(U_L) + F^-(U_R)$$

By applying FVS, the Euler equations become

$$\frac{\partial U}{\partial t} + \frac{\partial F^+}{\partial x} + \frac{\partial F^-}{\partial x} = 0 \quad (2.32)$$

In the above equation the positive flux is approximated using with the backward difference operator and the negative flux is approximated with the forward difference operator. There is no unique way of splitting the fluxes. We discuss one such FVS schemes due to van Leer [15] which we have used in our work in the subsequent sections.

2.3.2.1 van Leer scheme

van Leer has proposed a method of splitting the flux vector [15]. The mass momentum and energy fluxes were split such that the forward and backward fluxes transitioned smoothly at eigenvalue sign changes ie near sonic and stagnation points. The flux $F(W)$ with $W = (\rho, a, M)^T$ is split into a forward flux

$F^+(W)$ and a backward flux $F^-(W)$ as follows:

$$F_{\perp}(W) = F_{\perp}^+(W_R) + F_{\perp}^-(W_L) \quad (2.33)$$

with the local algebraic mach number $M_{\perp} = u_{\perp}/a$,

$$F_{\perp}^+ = \frac{\rho a}{4} (M_{\perp} + 1)^2 \begin{bmatrix} 1 \\ \frac{n_x[(\gamma-1)u_{\perp}+2a]}{\gamma} - n_y u_{||} \\ \frac{n_y[(\gamma-1)u_{\perp}+2a]}{\gamma} + n_x u_{||} \\ \frac{[(\gamma-1)u_{\perp}+2a]^2 + u_{||}^2}{2} \end{bmatrix} \quad (2.34)$$

$$F_{\perp}^- = -\frac{\rho a}{4} (M_{\perp} - 1)^2 \begin{bmatrix} 1 \\ \frac{n_x[(\gamma-1)u_{\perp}-2a]}{\gamma} - n_y u_{||} \\ \frac{n_y[(\gamma-1)u_{\perp}-2a]}{\gamma} + n_x u_{||} \\ \frac{[(\gamma-1)u_{\perp}-2a]^2 + u_{||}^2}{2} \end{bmatrix} \quad (2.35)$$

2.3.3 Flux Difference Splitting(FDS)

They fall into the category of solving the approximate Riemann solvers. In FDS schemes, the flux difference is split into *upwind* components. Here, the flux difference (ΔF) is split into a *positive part* and a *negative part* such that the positive part contains all the positive eigenvalues and the negative part contains all the negative eigenvalues .

$$\Delta F = (\Delta F)^- + (\Delta F)^+. \quad (2.36)$$

As in the FVS schemes, there is no unique way splitting the flux difference. Different schemes have been proposed based on the method of splitting . we discuss one such method due to Roe[16] which is used in this work.

2.3.3.1 Roe scheme

Roe has proposed a FDS scheme which is named after him [16]. According to his scheme,

$$dF = AdU \quad (2.37)$$

The finite difference analogue of the above differential relation is ,

$$\Delta F = \hat{A} \Delta U \quad (2.38)$$

where,

$$\Delta F = F_R - F_L \quad (2.39)$$

$$\Delta U = U_R - U_L \quad (2.40)$$

In the above equation subscripts R and L represent the right and left states respectively. Roe[16] has given the methodology for the construction of \hat{A} called the Roe averaged matrix. Expressing \hat{A} in the Jordan canonical form,

$$\Delta F = \hat{R} \hat{\Lambda} \hat{L} \Delta U \quad (2.41)$$

By introducing $\Delta \Psi = \hat{L} \Delta U$,

$$\Delta F = \hat{R} \hat{\Lambda} \Delta \Psi \quad (2.42)$$

or,

$$\Delta F = \sum_{i=1,3} \lambda_i \vec{r}_i \Delta \Psi_i \quad (2.43)$$

Now the term ΔF is split into two parts $(\Delta F)^-$ and $(\Delta F)^+$, which are the fluctuations corresponding to the backward moving waves and the forward moving waves respectively. This is done as follows:

$$(\Delta F)^- = \sum_{\lambda_i < 0} \lambda_i \vec{r}_i \Delta \Psi_i \quad (2.44)$$

and,

$$(\Delta F)^+ = \sum_{\lambda_i > 0} \lambda_i \vec{r}_i \Delta \Psi_i \quad (2.45)$$

Therefore it is possible to calculate the flux at the interface F_I using one of the formulas given below:

$$F_I = F_L + (\Delta F)^- \quad (2.46)$$

$$F_I = F_R - (\Delta F)^+ \quad (2.47)$$

Generally the the interfacial flux is expressed in terms of the symmetric formula obtained by taking average of the fluxes obtained using the above two formulas.

That is,

$$F_I = \frac{1}{2}(F_L + F_R) - \frac{1}{2} \sum_{i=1,3} \tilde{\tau}_i | \lambda_i | \Delta \Psi_i \quad (2.48)$$

The flux function of Roe [16] reads,

$$F_{\perp}(W_R, W_L) = \frac{1}{2}(F_{\perp}(W_R) + F_{\perp}(W_L)) - \frac{1}{2} | A(W_R, W_L, \hat{n}) | (W_R - W_L) \quad (2.49)$$

where, $A(W_R, W_L, \hat{n})$ is the Jacobian matrix defined using Roe's average:

$$< \rho > = \frac{\sqrt{\rho_R} \rho_R + \sqrt{\rho_L} \rho_L}{\sqrt{\rho_R} + \sqrt{\rho_L}} \quad (2.50)$$

$$< \vec{u} > = \frac{\sqrt{\rho_R} \vec{u}_R + \sqrt{\rho_L} \vec{u}_L}{\sqrt{\rho_R} + \sqrt{\rho_L}} \quad (2.51)$$

$$< H > = \frac{\sqrt{\rho_R} H_R + \sqrt{\rho_L} H_L}{\sqrt{\rho_R} + \sqrt{\rho_L}} \quad (2.52)$$

2.4 Summary

In this Chapter, we have discussed the basic ideas of Finite Volume Schemes, The Least Square Method, which has been discussed is useful in obtaining the gradient terms. Two important methods of obtaining the fluxes on the Cell interfaces such as Flux Vector Splitting Scheme and the Flux Difference Scheme have been discussed. The van Leer Scheme which is a FVS Scheme or the Roe Scheme which is a FDS Scheme is applied in conjunction with the Mirror or Mixed Boundary Condition in the various test cases that are carried out. These Boundary Conditions are discussed in the subsequent Chapters.

Chapter 3

Wall Boundary Conditions

A lot of work has already been done on finding of fluxes for the interior edges. But not much attention was given to the Wall Boundary Conditions. For the Computation of many Fluid Dynamic problems more difficulty is encountered in satisfying the Boundary Conditions than in balancing the Differential Equations at the interior points of the flow field. This is so because on the Boundary not all the flow Variables are specified by the Boundary Conditions, and there remain more unknowns than the interior Equations. The problem is fully defined only when the proper Boundary Conditions are specified. The Boundary Conditions are such an important part of the Problem that the pattern of the two flow fields can be completely different from one another because of some differences in the flow boundaries, despite the fact that both Flows obey the same system of Partial Differential Equations. Flow essentially develops its characteristics because of what happens on the Boundaries. Thus Wall Boundary Conditions becomes important.

From the theory of characteristics, at any boundary, the variables corresponding to the outgoing and incoming information must be identified. Only the variables corresponding to the information transported from the boundary towards the interior(*incoming*) can be freely imposed as *physical boundary con-*

ditions. All other variables which correspond to the outgoing information must be evaluated from the interior information which are called *numerical boundary conditions*. As for as the solid wall is considered, only one characteristic enters the flow domain from outside and the rest of the characteristics leave the flow domain. Refer fig 3.1. Therefore it is necessary to provide only one information on the wall based on the physical considerations as *natural boundary conditions*. This condition is expressed by the vanishing normal velocity.

$$u_{\perp} = 0 \quad (3.1)$$

As a result all the convective components through the solid wall will vanish in

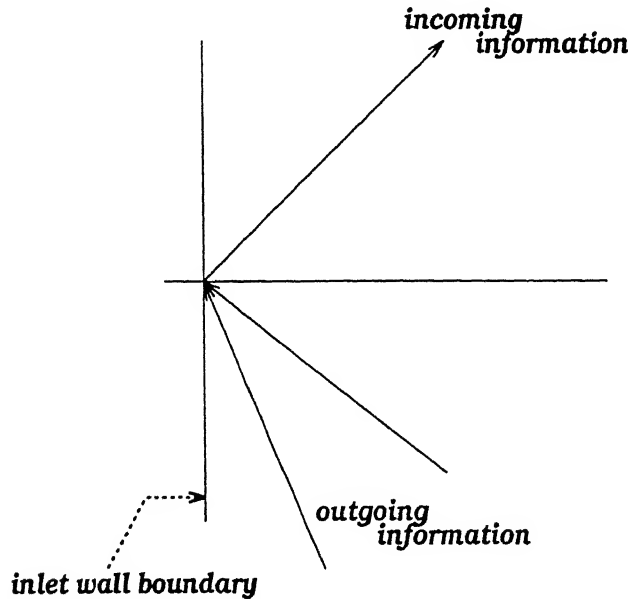


Figure 3.1: Directions of information flow at the Wall boundary

the computation of the flux terms and the flux vector reduces to the following

expression in a 2-D flow.

$$F_{\perp B} = \begin{bmatrix} 0 \\ p\hat{n}_x \\ p\hat{n}_y \\ 0 \end{bmatrix} \quad (3.2)$$

Hence, only the pressure component remains at the wall. So, in the Finite Volume schemes, only Pressure is required for calculating Fluxes on the Wall Boundary Conditions.

As we stated earlier, there are two ways of implimenting the Wall boundary conditions. One of them is the *Strong formulation* while the other is the *weak formulation*. In the following section, we present the strong formulation in detail which is followed by the weak formulation.

3.1 Strong formulation

In the strong formulation, the zero normal velocity on the wall is enforced explicitly, ie state variables on the wall boundary are defined using the physical constraints which are explained in this section later, where as the state variables at the interior nodes are updated using the Finite Volume state update formula(eq.no 2.4).

As we stated earlier, at the wall boundary, only one information has to be provided explicitly at the wall. Naturally this condition will be

$$u_{\perp} = 0 \quad (3.3)$$

The second physical constraint corresponds to the normal momentum

equation for the rigid stationary walls satisfying $\frac{\partial u_{\perp}}{\partial t} = 0$ and is given by

$$\frac{\partial p}{\partial n} = -\rho \frac{u_{\parallel}^2}{R} \quad (3.4)$$

where ρ is the mass density, u_{\parallel} is the tangential velocity and R is the radius of curvature. But the use of the radius of curvature in the above equation can be avoided simply by using the differential relation obtained from the non conservative form of Euler equations.

$$\frac{\partial p}{\partial n} = -\rho \hat{n} \cdot ((\vec{u} \cdot \nabla) \vec{u}) \quad (3.5)$$

It is also possible to obtain a similar relation for the normal gradient of pressure on the Wall using the conservative form of Euler equations. One more way of determining the pressure on the wall satisfying the normal momentum equation is to use the conservative integral relation [20],

$$\int_{\partial\Omega_B} F_{\perp} ds = - \int_{\partial\Omega_I} F_{\perp} ds \quad (3.6)$$

Here, Ω_B and Ω_I represent the boundary and the interior edges of any wall boundary cell respectively. Assuming that the pressure is constant along the boundary edges of each cell of the wall boundary cells, we have the following relation for the pressure on the boundary,

$$p_B = -\frac{1}{\Delta s_B} \left[n_x \int_{\partial\Omega_I} F_{\perp 2} ds + n_y \int_{\partial\Omega_I} F_{\perp 3} ds \right] \quad (3.7)$$

where, Δs_B is the length of the boundary edge. In our work we have used (eqn no.3.7) for satisfying the normal momentum equation on the wall. The third physical constraint used, is the Crocco's relation [19]. Crocco's relation in a direction normal to the wall is given by

$$\frac{\partial S}{\partial n} = -\frac{\gamma-1}{\rho^{\gamma-1}} u_{\parallel} \omega \quad (3.8)$$

where, $S = p/\rho^{\gamma}$ is an entropy like variable. Here isentropy of the flow is assumed. In the case of inviscid subsonic flows without discontinuities, this relation becomes,

$$\frac{\partial S}{\partial n} = 0 \quad (3.9)$$

The computations in this work are based on the (eqn.no.3.9). Enforcing the normal entropy gradient on the wall boundary has been found less dissipative for subsonic and transonic flows. The computations in this work, constraint (eqn.no.3.9) is used in preference to (eqn.no.3.8). Even if the flow is irrotational(as in the subsonic test case), the vorticities computed on the wall are considerably high [1] because of the numerical errors. This problem is found to be even more acute in the stagnation regions. Therefore the use of such erroneous wall vorticities in the satisfaction of the entropy condition on the wall makes the boundary condition more dissipative. The fourth constraint used is related to the total enthalpy. ie Total enthalpy remains constant for the inviscid flows without source terms if the flow at infinity is isenthalpic. ie

$$\frac{\partial H}{\partial n} = 0 \quad (3.10)$$

where, $H = (E + p)/\rho$ is the total enthalpy. Thus the above equation can also be used as a constraint for obtaining the boundary conditions.

The values of any variable Φ (S,H or p as the case may be) on the wall can be obtained by enforcing the conditions on the normal gradients using the Method of Least Squares ie (eqn. no. 2.13).

The main advantage of the strong formulation is that it is less dissipative. It also takes into account, the curvature effects of the wall boundary. The curvature effects are taken care by the equation number 3.4. The main disadvantage of the strong formulation is that, the scheme used for the boundary points is different from the one that was used for the interior points. Therefore it violates global law of conservation. The other drawback of the strong formulation is that, its implementation is direct in the case of cell vertex finite volume framework where as in case of the cell center finite volume framework, it is not so. This is because, the reference point will be present on the boundary surface in the case of cell vertex framework where as, it is not so in the case of the cell center framework. Also in the case of the cell center framework,

the normal velocity is not zero at the reference points of the boundary cells. Hence, (eqn.no.3.1) is not valid in this case. For structured meshes this problem can be overcome by using the half cells at the wall boundary. Therefore it is necessary to design weak boundary conditions which take into account the curvature effects and also which are less dissipative.

3.2 Weak formulation

In the weak formulation, the natural boundary condition $u_{\perp} = 0$ is enforced through flux function. Therefore the weak boundary conditions reduce to the determination of fluxes at the cell interfaces coinciding with the boundary through the physical constraints. The reference points of the boundary are updated in a way similar to the interior cells. So contrary to the strong formulation, the implementation of the weak boundary conditions is same in both the cell center and cell vertex frameworks. Here, we are presenting Mirror boundary condition which we have used in our work which is later followed by the Mixed Boundary Condition in next section.

3.2.1 Mirror condition

In this boundary condition, the variables in the fictitious cells are defined such a way as to ensure the vanishing mass Flux at the wall. Once, the fictitious state are defined, the fluxes on the boundary edges are calculated based on the information obtained from the computational domain (interior state) on one side and the fictitious cells on the other. So, in this boundary condition the approximate Riemann solver used for determining the fluxes on the interior edges is used on the wall boundary also. There are various ways of defining the fictitious state. In our work we are using the reflection principle which guarantees the zero normal flux across the wall boundary. As the name

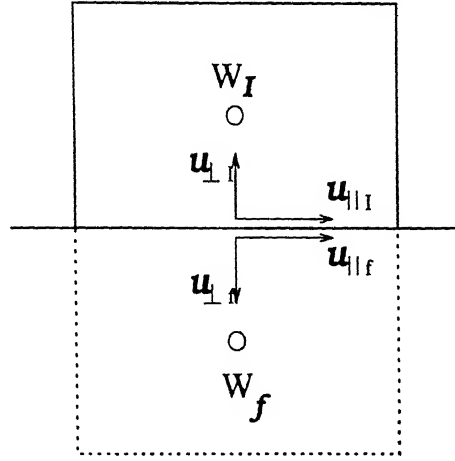


Figure 3.2: Mirror boundary condition

indicates the pressure, density and the tangential velocity of the interior cells are reflected on to the fictitious cells. To make the mass flux on the wall to be zero, the normal velocity in the fictitious cell is equal and opposite to that in the interior cell. Therefore the mirror condition is stated as follows:

$$\begin{aligned}
 u_{\perp f} &= -u_{\perp I} \\
 u_{\parallel f} &= u_{\parallel I} \\
 p_f &= p_I \\
 \rho_f &= \rho_I
 \end{aligned}
 \tag{3.11}$$

where, the subscripts I and f refer to the interior and fictitious states respectively.

The important advantage of the Mirror condition is that it permits the use of the interior scheme and thus the direction of information propagation is maintained at the boundary also. The main drawback of this boundary condition is that it is dissipative and it doesnot take into account the curvature effects.

3.3 Mixed Boundary Condition

It is clear from the above discussion that both the strong formulations and the weak formulations have their own merits and demerits. In order to harness the advantages of both the formulations, we are using the *Mixed boundary condition*. One of the ways incorporating the features of the Strong Formulation in the Weak Formulation is by making use of the constraints in the Equations numbered 3.3, 3.7, 3.8, 3.10 directly to obtain the wall fluxes. But such a procedure boils down to determining simply Pressure on the wall using the normal momentum equation. This is found to be unstable and leads to the development of artificial boundary layer on the wall. Therefore it becomes important to look into other ways of implementation and Mixed Boundary Condition is a result of such an outcome [1].

In this Mixed boundary treatment, we define the fictitious cells by using the strong formulation, that is by using the physical constraints stated in the strong formulation. The interior state is determined in a way similar to the Mirror Condition. Now both the states across the boundary edges are defined and so the approximate Riemann solver can be used to determine the wall fluxes.

It can be noted here that this boundary treatment is also not conservative, that is it allows the transpiration of the mass flux across the rigid wall boundary. But, the justification for the use of this treatment comes from the fact that the computed fluid velocities normal to the boundary wall at the steady state are very small. Numerical errors involved are also very small. Numerical results also confirm this fact.

3.4 Summary

In this Chapter, we have discussed the basic ideas of the different types of formulations used for the Wall Boundary Conditions. In the Strong formulation zero normal velocity on the Wall Boundary is enforced explicitly whereas, in the Weak Formulations, the same is done through the flux function. As an example for the Weak Formulation, we have also discussed about the Mirror Boundary Condition. Both these Schemes have their own advantages and the disadvantages. The Mixed Boundary Condition which takes into account the advantages of both the Strong and Weak Formulations, is expected to produce better results. Many numerical experiments have been performed to verify this fact. The results obtained with the Mirror Wall Boundary Condition have been compared with those obtained with the Mixed Wall Boundary Condition which is a Weak Formulation. These results have been discussed in next Chapter.

Chapter 4

Results and Discussions

The boundary conditions discussed in the earlier chapters have been tested for various test cases such as,

1. Subsonic flow past NACA 0012
2. Transonic flow past NACA 0012
3. Supersonic flow through an expansion channel

In the first two cases, van Leer, Roe and the Combination of both the schemes .i.e., Roe scheme for the interior cell and the van Leer scheme for the boundary cells have been used. The Mixed Boundary Condition used in conjunction with the FDS doesnot seem to improve the quality of the results significantly [1]. Therefore a combination of FDS scheme for the interior edges and the FVS scheme for the boundary edges has been carried out in this work.

The details regarding the grids that are used for the various computations are presented in the table 4.1. All the grids are symmetric regular quadrilateral grids. These grids are shown in fig.4.1. In order to extract the information at the walls properly, the number of grids at the wall have been increased. In the

results presented, the wall entropy deviation is defined as,

$$\Delta S = \left[\frac{p}{p_\infty} \left(\frac{\rho_\infty}{\rho} \right)^\gamma - 1 \right] \quad (4.1)$$

All the computations were made using either van Leer or Roe's Scheme.

Table 4.1
Grid details

<i>Name</i>	<i>configuration</i>	<i>Nodes</i>	<i>cells</i>	<i>Edges</i>
Grid1	Airfoil NACA0012	2112	2048	4160
Grid2	Expansion channel	2821	2700	5520

4.1 Subsonic flow past NACA 0012

This is one of the standard GAMM [16] test cases for evaluating different schemes for the subsonic flows. The free stream Mach no is 0.63 and the angle of attack is 2.0.

Mach contours obtained by using van Leer Scheme are shown in fig4.2. The wall entropy generated for the same case are presented in the fig.4.3. The entropy layer generated by the wall boundary condition becomes apparent when we look at the Mach contours. It is also clear from the wall entropy plots. The wall entropy generated in the case of Mirror Boundary Condition is in the range of 0.01 to 0.04 whereas that in the case of Mixed Boundary Condition, it is in the range of 0.005 to 0.02. So, clearly the entropy generated by the Mirror Boundary Condition is higher than that generated by the Mixed Boundary Condition.

The Mixed Boundary Condition used in conjunction with the FDS Schemes such as Roe, doesnot seem to improve the results significantly over the Mirror

Boundary Condition [1]. In order to extend the applicability Mixed boundary condition for the FDS schemes, we have tried using the FDS schemes for flux calculation of the interior edges and FVS schemes for flux calculation of the boundary edges. The Mach contours are shown in fig.4.4. The entropy generation at the wall is plotted in the fig.4.5. As seen in the earlier case, the Mach contours obtained using the Mixed Boundary Condition are superior to those obtained using the Mirror Boundary Condition. Again, as seen earlier, the Mach contours in this case also clearly shows the superiority of the Mixed Boundary Condition over the Mirror Boundary Condition. This is again confirmed by the wall entropy changes which show that the wall entropy in the case of Mirror Boundary Condition are much higher than that in the case of Mixed Boundary Condition.

The above results show that the entropy generated on the wall due to Boundary Condition in the stagnation region was high irrespective of the type of wall Boundary Condition. The entropy generation due to mirror Boundary Condition was high as compared to that of the Mixed Boundary Condition. In the stagnation region the gradients with the flow field high. As a result, the numerical dissipation will also be more in this region. So, the Vortices generated in this region are also high. These Vortices are convected downstream towards the leading edge. To reduce the Vorticity generation in the stagnation region, either a fine grid or a numerically less dissipative wall boundary condition should be used. By following the latter method, we have used the Mixed boundary condition which is less dissipative in the stagnation region and the Mirror boundary condition downstream.

The mach contours and the wall entropy obtained are shown in fig.4.6. The Mach contours shows a clear improvement over the Mirror conditions, though may not be better than the Mixed Boundary Condition of the van Leer scheme. The wall entropy plot confirms this fact much more clearly. But, the experiment produces oscillations in the wall entropy generated at the

stagnation region. This is not desirable. This is mainly because of the sudden switch from the Mixed wall Boundary Condition to the Mirror wall boundary condition which are not smooth.

4.2 Transonic flow past NACA 0012

In this case, the Mach number is 0.8 and the angle of attack is 1.25. This is one of the standard cases of AGARD [17]. This is a very interesting test case, because this has a shock in the upper surface and a relatively weaker shock, (closer to the leading edge than the upper shock) on the lower surface of the airfoil. It is generally possible to capture the upper surface shock accurately, but capturing the lower surface shock is difficult(AGARD[17]). The results of the transonic flow cases follow the lines of the subsonic flow which were shown in the earlier sections.

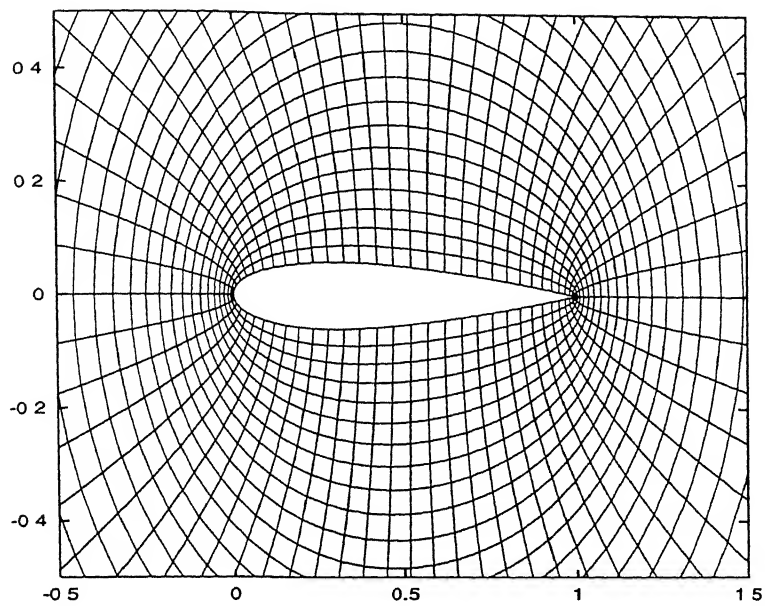
The Mach Contours obtained by using van Leer Scheme are presented in fig.4.7. and the wall entropy plots are presented in fig.4.8. This fact is also confirmed when we look at the wall entropy plots which show that the entropy generated at the wall (which is purely numerical) due to the Mirror wall boundary condition is high as compared to that due to the Mixed wall boundary condition.

Similar to the subsonic flows, to get the improved results for the Roe scheme, computations were done using the van Leer Scheme at the wall and Roe scheme in the interior cells. The results as expected, showed improvement. The Mach contours, and the wall entropy plots are shown in fig.4.9 and fig.4.10 respectively. Both the plots confirm the superiority of Mixed wall boundary condition over the Mirror wall boundary condition.

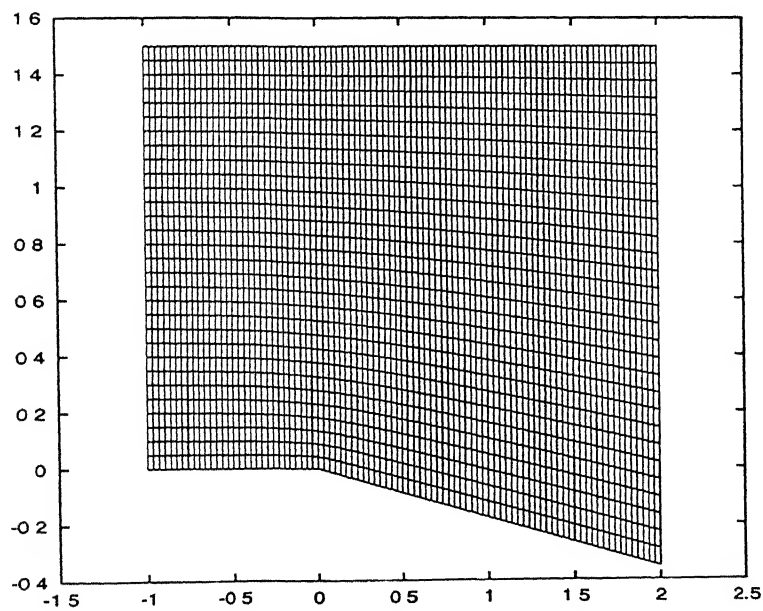
4.3 Supersonic Flow Through an Expansion Channel

In this case the free stream Mach number is 2.0. This is a very interesting case since, there will be an expansion fan at the change of cross section. This is an isentropic phenomenon [19]. As a result, there will not any entropy generation along the Wall. So, any entropy generation in the computations for this case will be purely numerical in nature. The Mach Contours obtained for this case are presented in fig.4.11. The Wall entropy along the Wall are shown in fig.4.12a. Though the Mach Contours donot show any difference between the two types of Wall boundary condition, the entropy plots highlights the difference. They clearly show that the entropy generation due to the Mirror Wall boundary condition is more as compared to that due to the Mixed Wall boundary condition, thus confirming the superiority of the Mixed Wall boundary condition over the Mirror Wall boundary conditions.

It has been established that the strong formulation is less dissipative [1]. As stated in the earlier sections, the Mixed Wall boundary condition makes use of the strong formulation to determine the fictitious state. The strong formulation takes into account the curvature effect. Then the interior state is determined in a way similar to the Mirror condition. The mirror boundary condition, as we stated earlier, does not take into account the curvature effects and also it is dissipative. The first order computations of Mirror conditions in case of finite volume, will have variables at the walls same as the cell values themselves. Therefore, these wall boundary condition assumes the zero normal pressure and density gradients on the wall and thus violates Crocco's relation and momentum equation. When a higher order reconstruction procedure is adopted, though the spatial variations of the variables are properly represented, numerical experiments indicate that this alone is inadequate to make the Mirror boundary condition less dissipative.

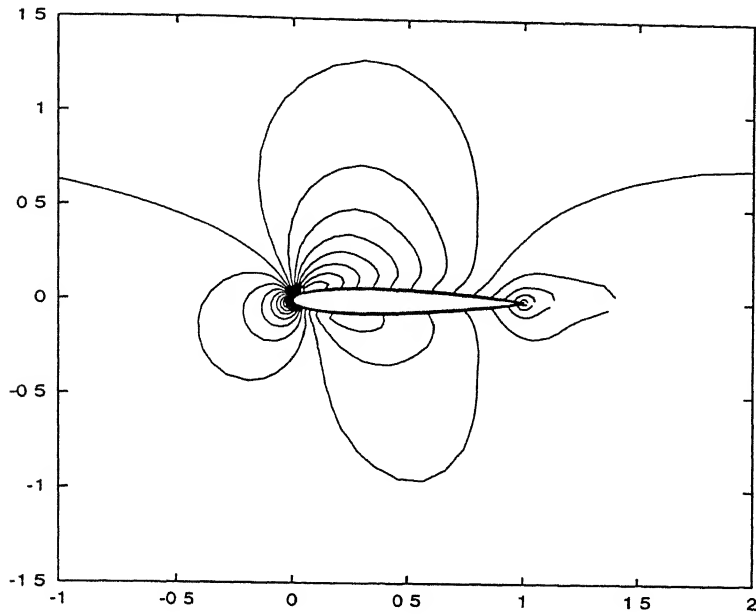


(a) Grid1:Airfoil NACA0012

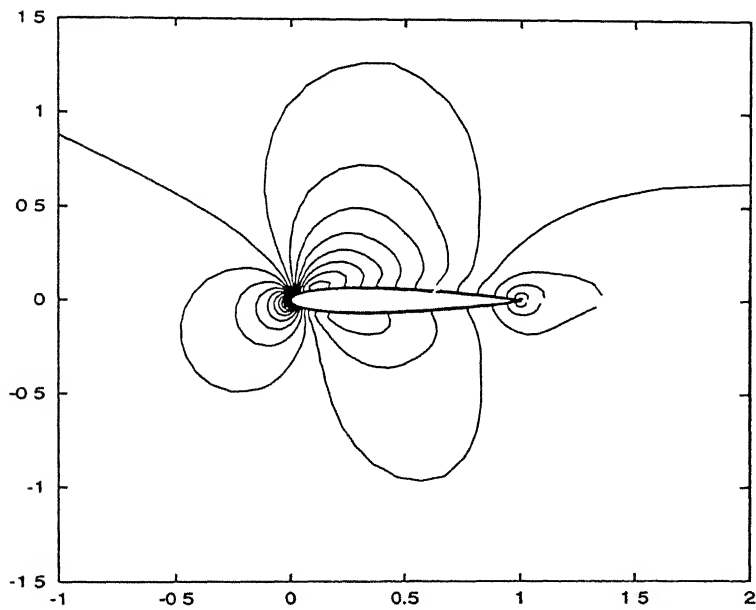


(b) Grid2:Expansion channel

Figure 4.1: Grids used

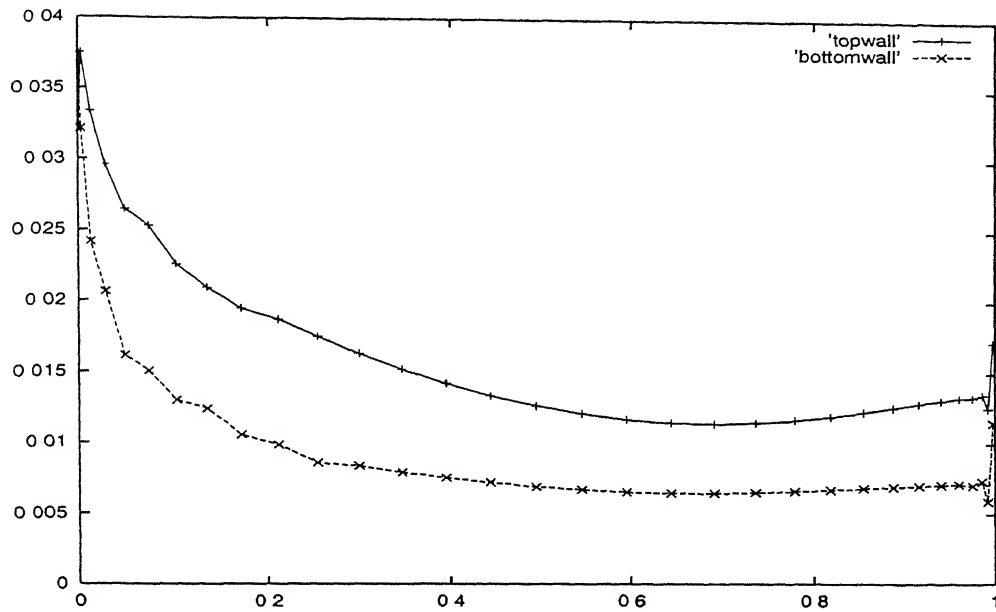


(a) Mirror Wall Boundary Condition

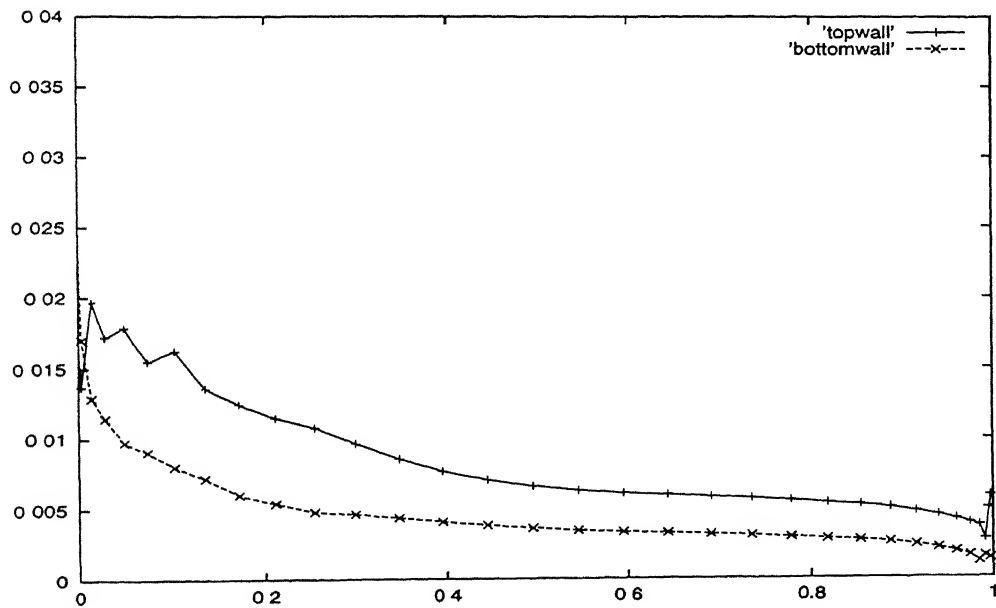


(b) Mixed Wall Boundary Condition

Figure 4.2: MACH CONTOURS WITH VAN LEER SCHEME (Mach No. = 0.63 and Alpha = 2.00 degrees)

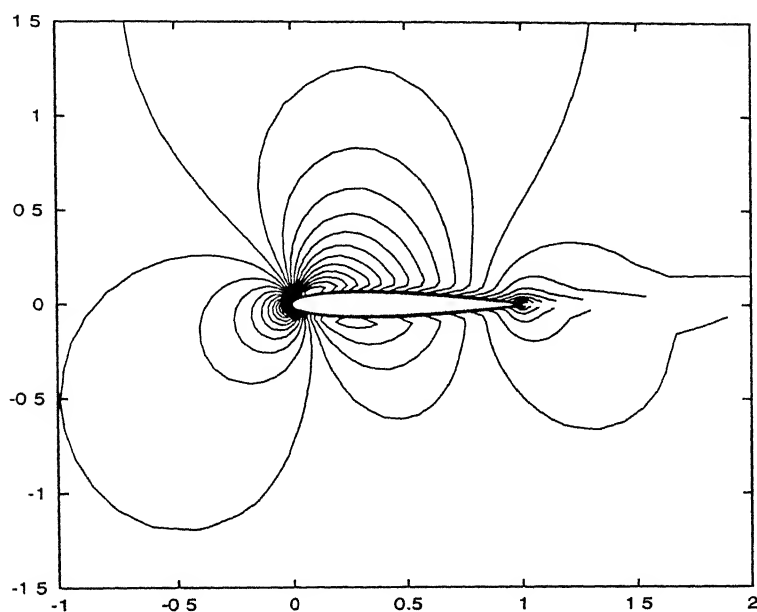


(a) Mirror Wall Boundary Condition

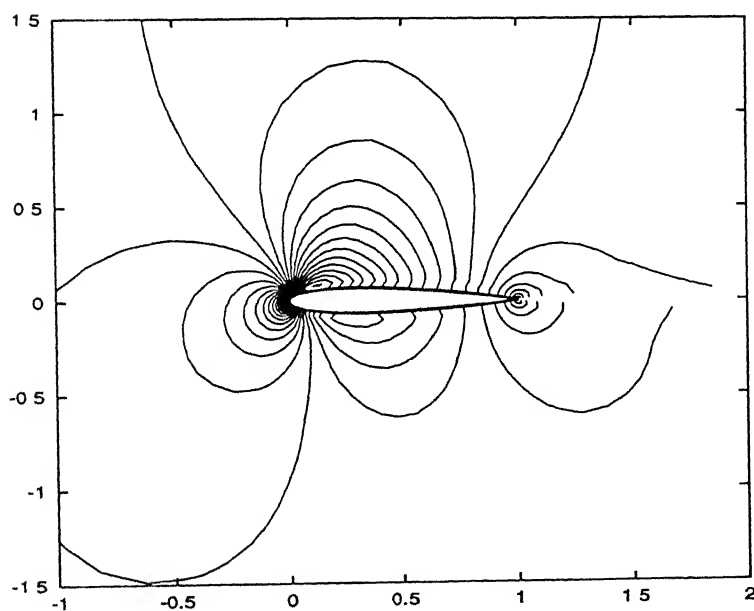


(b) Mixed Wall Boundary Condition

Figure 4.3: WALL ENTROPY FOR THE VAN LEER SCHEME (Mach No = 0.63 and Alpha = 2.00 degrees)

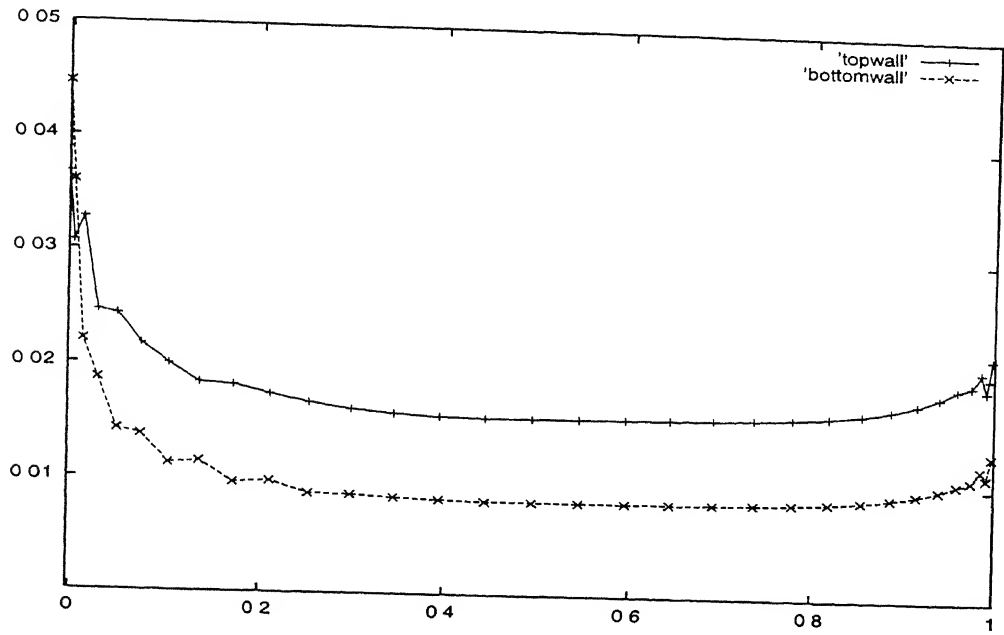


(a) Mirror Wall Boundary Condition

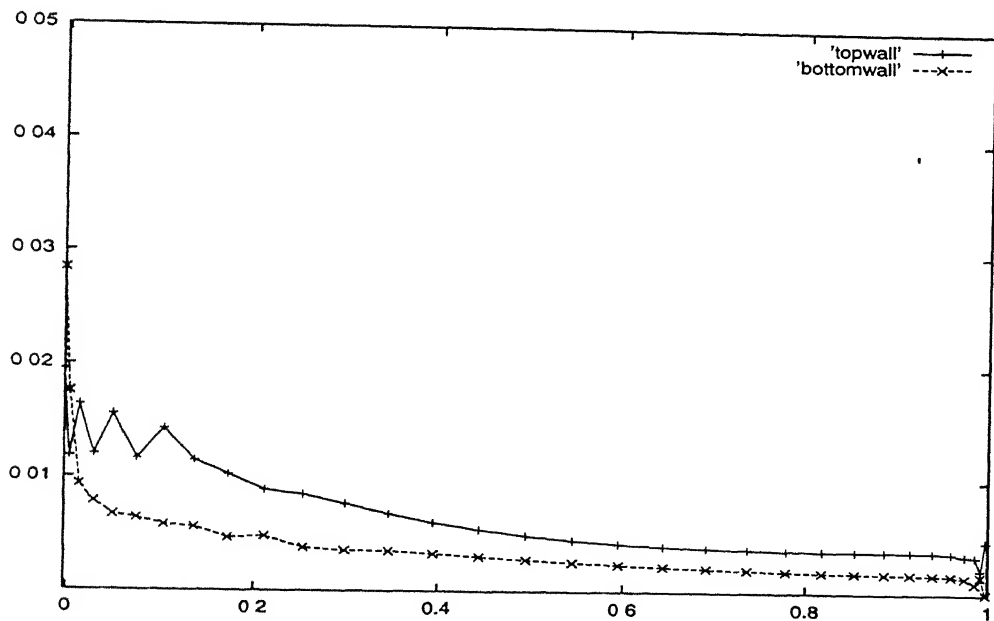


(b) Mixed Wall Boundary Condition

Figure 4.4: MACH CONTOURS WITH ROE-LEER SCHEME (Mach No. = 0.63 and Alpha = 2.00 degrees)

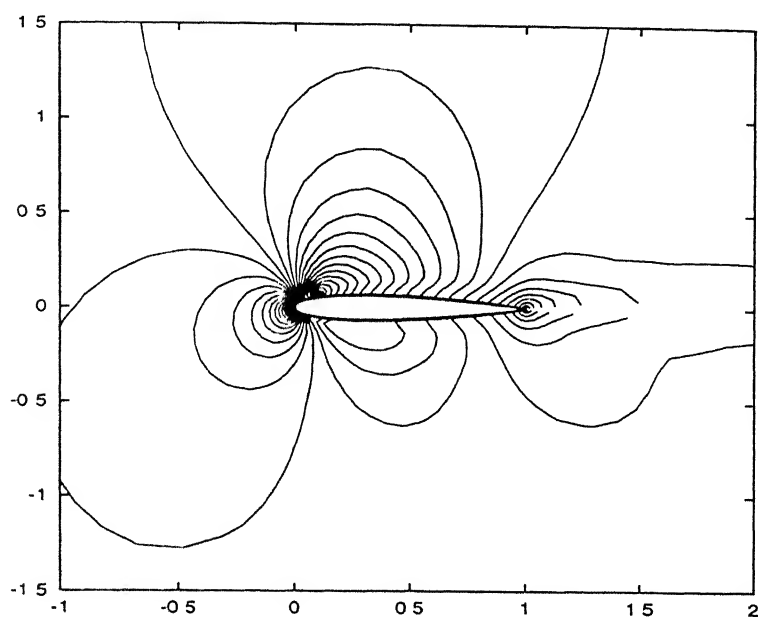


(a) Mirror Wall Boundary Condition

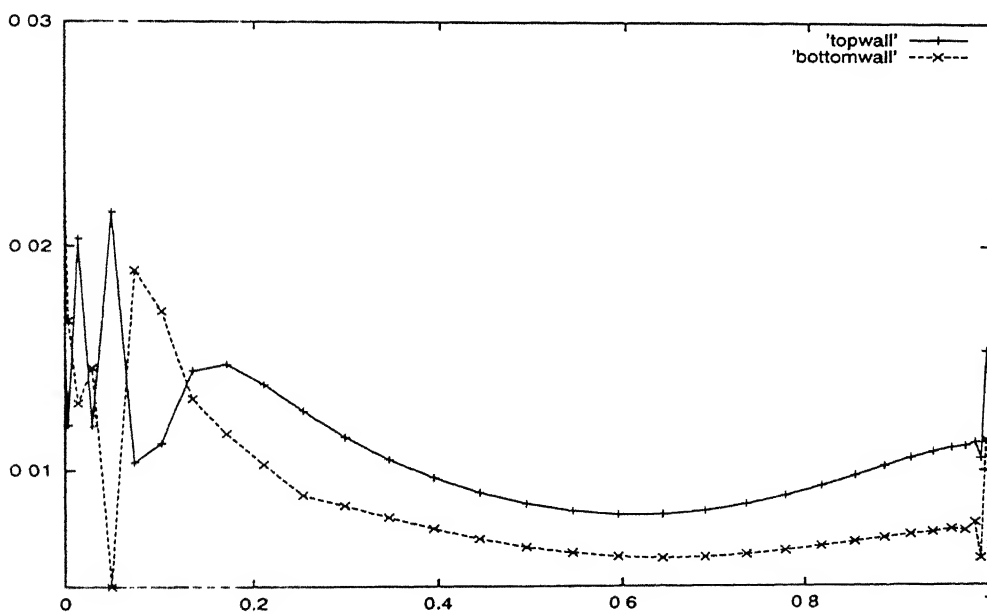


(b) Mixed Wall Boundary Condition

Figure 4.5: WALL ENTROPY FOR THE ROE-LEER SCHEME (Mach No = 0.63 and Alpha = 2.00 degrees)

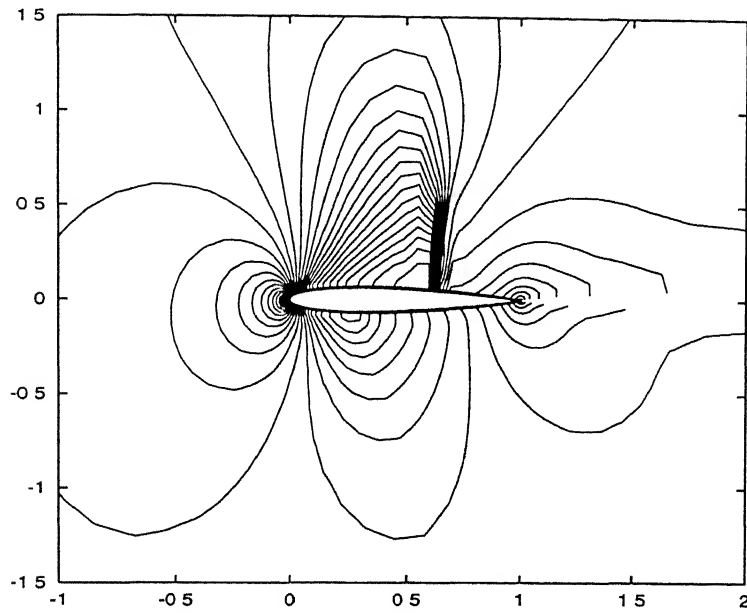


(a) Mach contours with the van Leer scheme

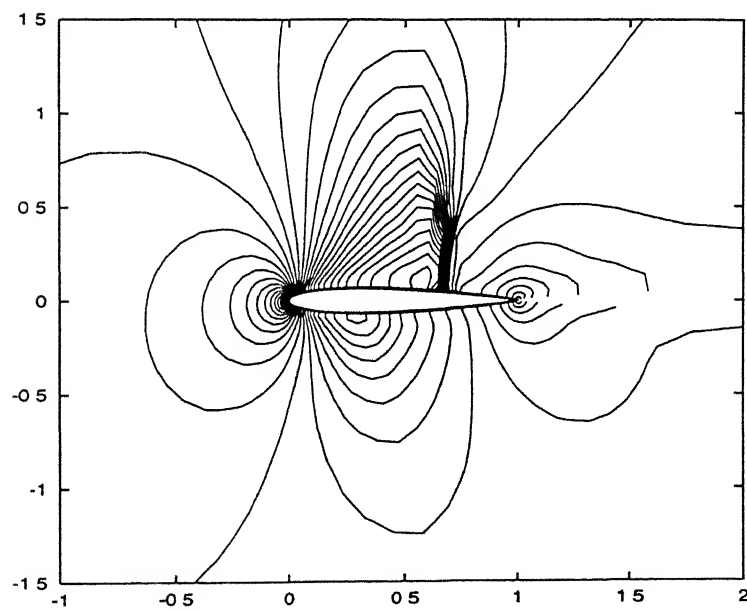


(b) Wall entropy with the van Leer scheme

Figure 4.6: MIXTURE OF MIRROR AND MIXED BOUNDARY CONDITION

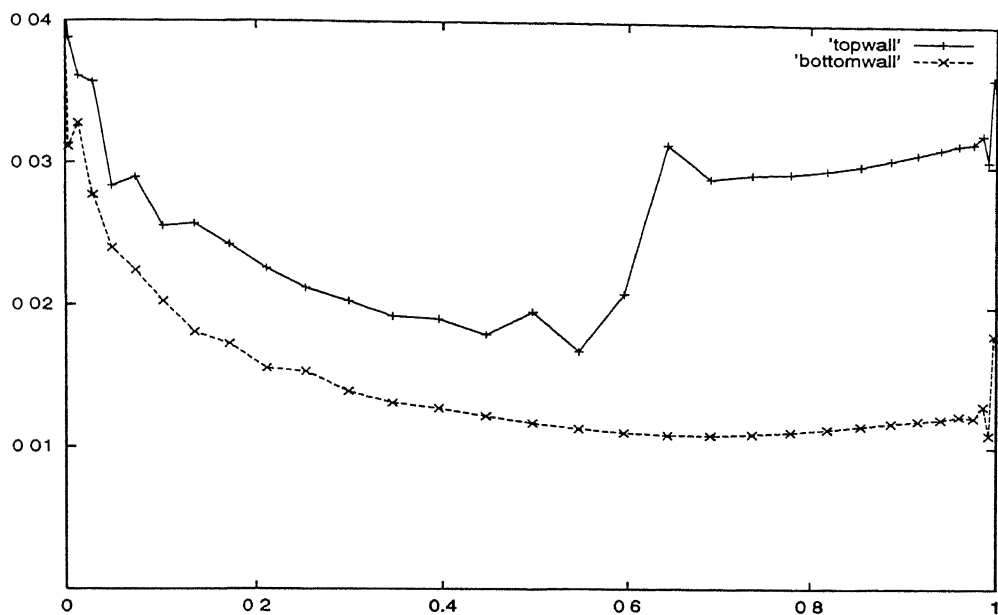


(a) Mirror Wall Boundary Condition

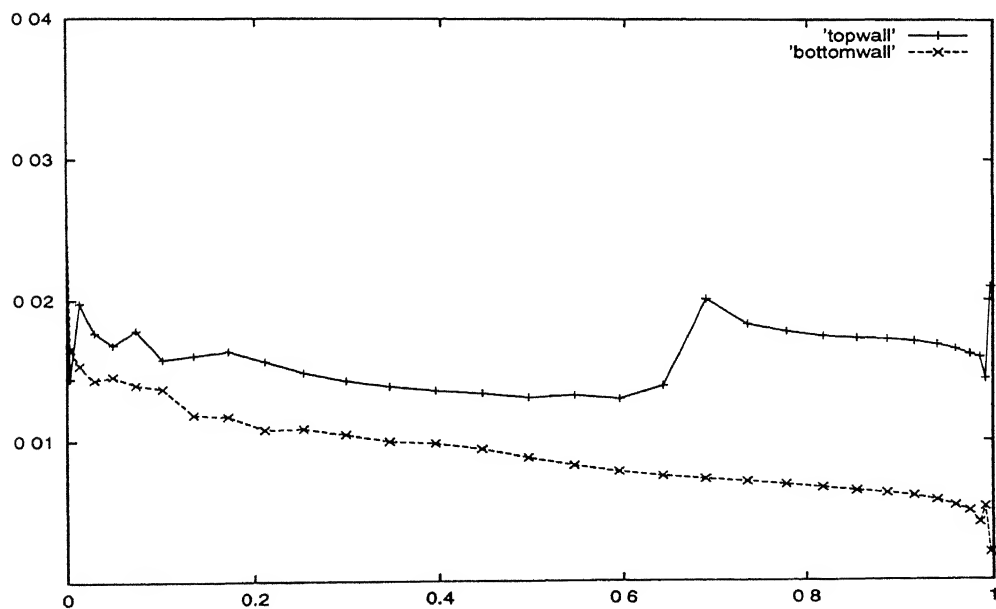


(b) Mixed Wall Boundary Condition

Figure 4.7: MACH CONTOURS WITH LEER SCHEME (Mach No. = 0.8 and Alpha = 1.25 degrees)

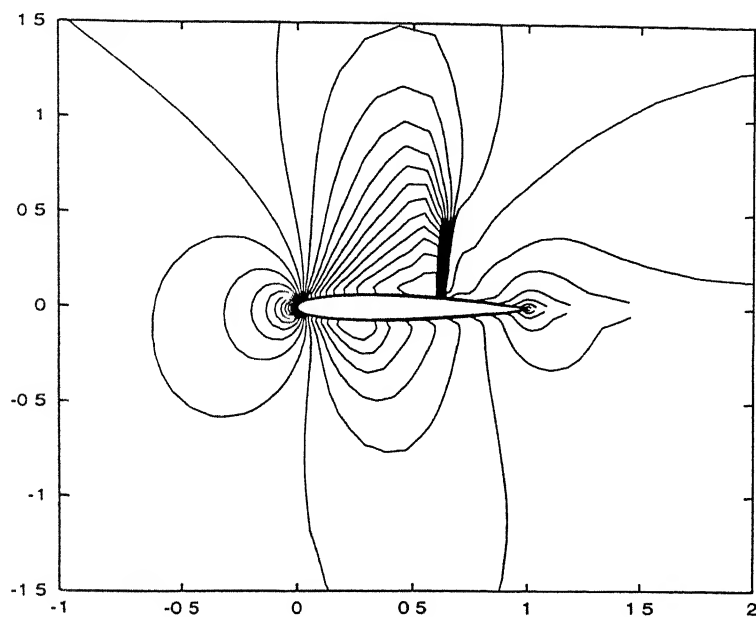


(a) Mirror Wall Boundary Condition

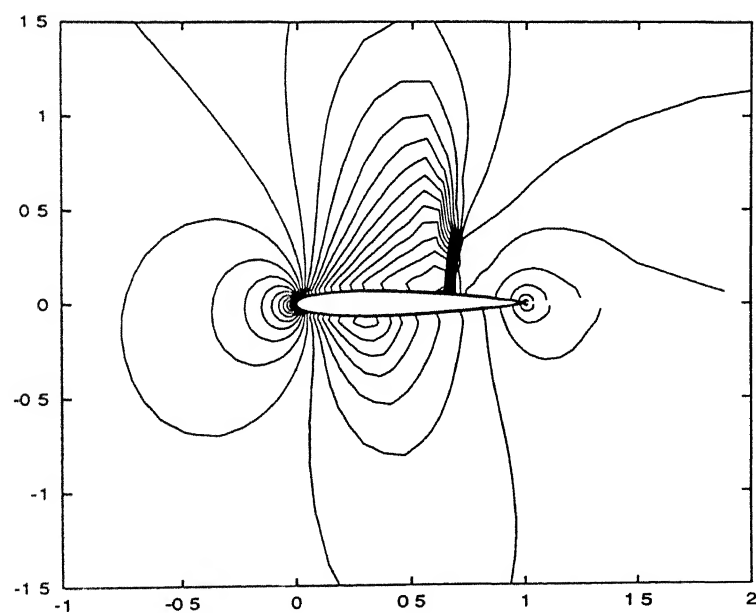


(b) Mixed Wall Boundary Condition

Figure 4.8: WALL ENTROPY FOR THE LEER SCHEME (Mach No = 0.8 and Alpha = 1.25 degrees)

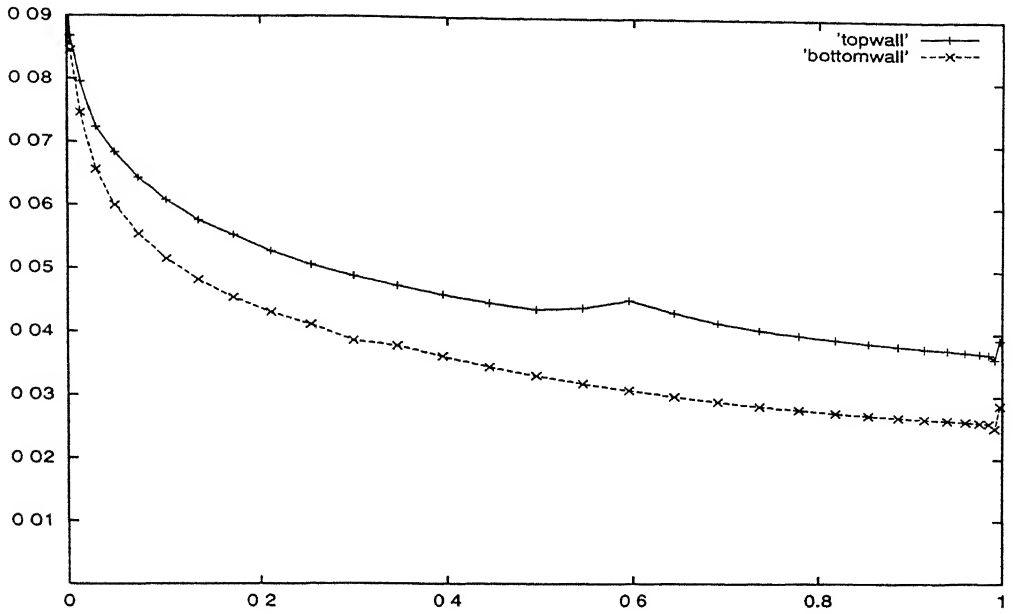


(a) Mirror Wall Boundary Condition

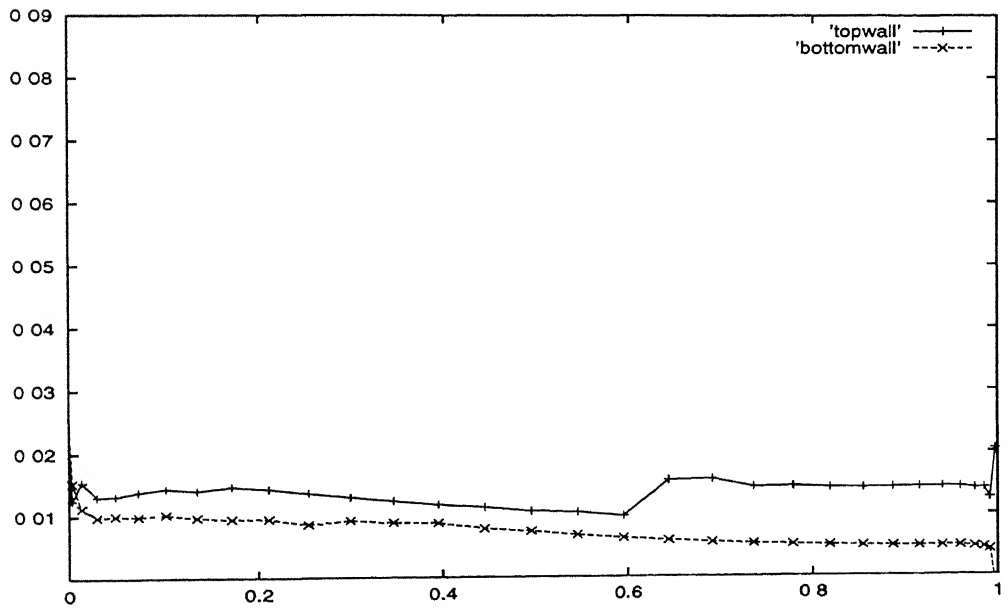


(b) Mixed Wall Boundary Condition

Figure 4.9: MACH CONTOURS WITH ROE-LEER SCHEME (Mach No. = 0.8 and Alpha = 1.25 degrees)

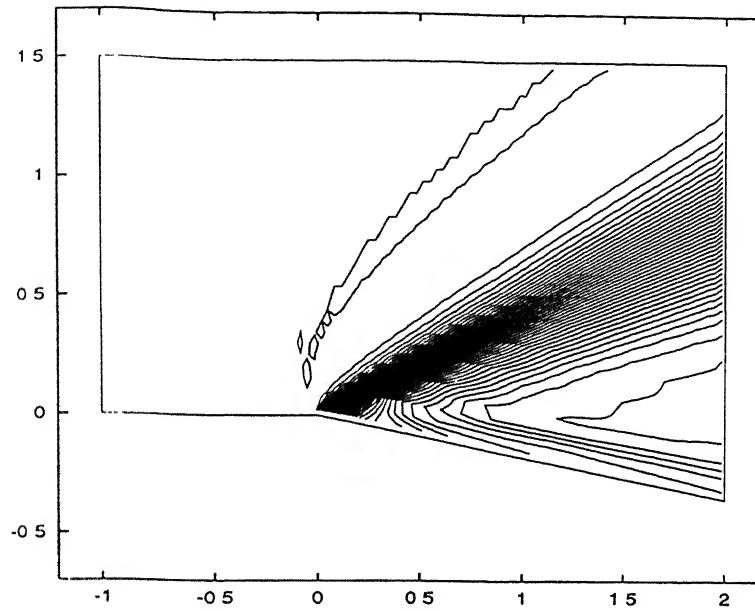


(a) Mirror Wall Boundary Condition

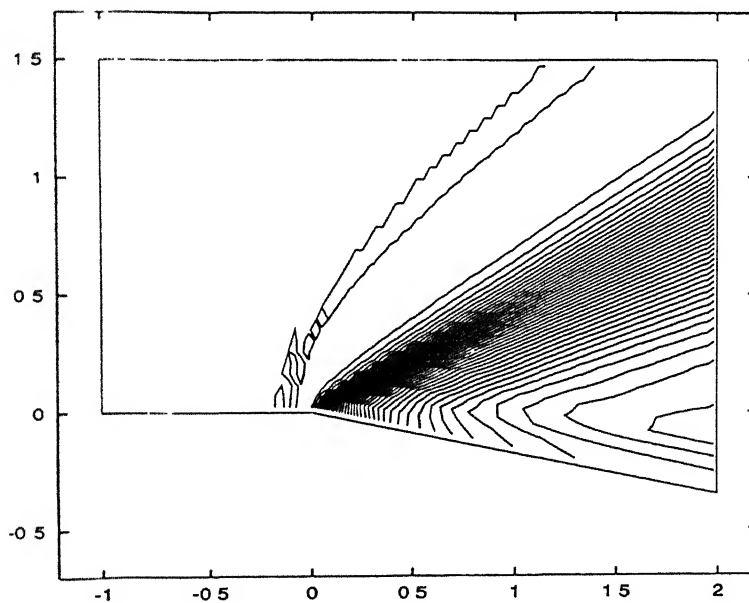


(b) Mixed Wall Boundary Condition

Figure 4.10: WALL ENTROPY FOR THE ROE-LEER SCHEME (Mach No = 0.8 and Alpha = 1.25 degrees)



(a) Mirror Wall Boundary Condition



(b) Mixed Wall Boundary Condition

Figure 4.11: MACH CONTOURS WITH VAN LEER SCHEME (Mach No. = 2.0)

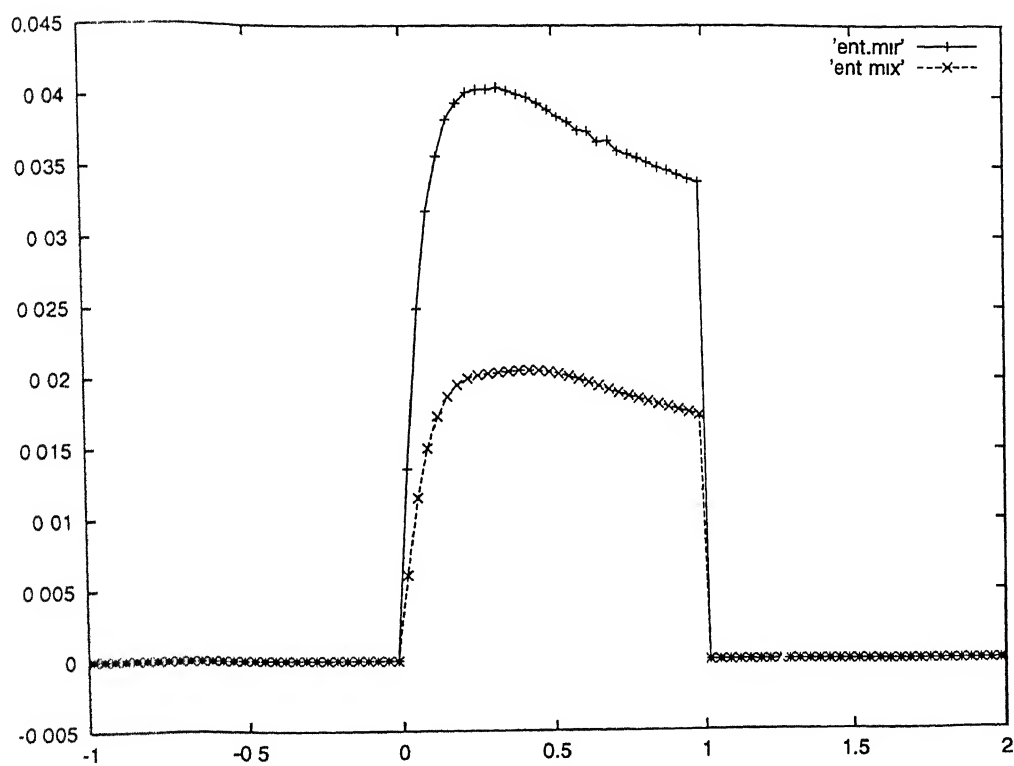


Figure 4.12: WALL ENTROPY COMPARISON

Bibliography

- [1] Balakrishnan, N and Fernandez, G "*Wall Boundary Conditions for Inviscid Compressible Flows on unstructured Meshes*", Submitted to the international Journal on Numerical methods in Fluid Dynamics, 1996
- [2] Lax, P.D. and Wendroff, B, "*Difference Schemes for Hyperbolic Equations with Higher Order Accuracy*", Comm. pure and Appl. Math. , Vol. 17, p 381-398.
- [3] Mac Cormack, R.W., "*Numerical Solution of the interaction of a Shock Wave with a Laminar Boundary Layer*", Proceedings of the Second International Conference on Numerical methods in Fluid Dynamics, Lecture Notes in Physics, Vol. 414, p 115-119, Springer-Verlag, New York.
- [4] Jameson, A, "*Artificial Diffusion, Upwind Biasing, Limiters and their Effect on Accuracy and Multigrid Convergence in Transonic and Hypersonic Flows*", AIAA-93-3359
- [5] Deconick, H and Struijs, R, "*Consistent Boundary Conditions for cell centered upwind Finite Volume Euler solvers* ", Num, Meth. for Dynamics-3, Clarendon Press, Oxford 12/CFD, April 1988.
- [6] Chakravarthy, R, "*Euler Equations-Implicit Schemes and BCs*", AIAA Journal, Vol.21, NO.

- [7] Butler, D.S, "*Characteristics in three independent Variables, Numerical solutions of ordinary and PDEs*", ed.L.Fox, Addison-wesley, New York 1962.
- [8] Porter, R.W.; Coakley, J.F., " *Use of Charecteristics for boundaries in time dependent finite difference analysis of multidimensional gas dynamics*" , Internat. J. Numer. Meth. Engng. 5,91-101 (1972)
- [9] Mac Cormack, R.W, Paullay, A.J., "*The influence of computational mesh on accuracy for initial value problems with discontinuous or nonunique solutions*, Computers and Fluids,2,339-361(1974).
- [10] Rizzi,A.W , Bailey,H.E, "*Finite Volume Solutions of Euler equations for steady three-dimensional transonic flow*", Proc. Fifth Internat. Conf. on Numer. Methods in Fluid Dynamics,eds. A.I.Vander Vooren and P J. Zandbergen, Lecture Notes in Physics, 59, springer-Verlag, pp. 347-357 (1976)
- [11] Rizzi A., "*Numerical Implementation of solid-body Boundary Conditions for Euler equations*, Z.A.M.M., Band 58, heft 7, pp. T301-T304,1978.
- [12] Moretti G., " *Importance of Boundary Conditions in Numerical t of Hyperbolic Equations*", Proceedings of the International Symposium on High speed Computing in Numerical Fluid Dynamics, Monterey, 1968.
- [13] Anderson, W.K. and Van Leer,B., "*A comparison of Finite Volume Vector Splittings for Euler Equations*", AIAA 23rd Aerospace Science Meeting, Jan. 14-17, Reno, Nevada.
- [14] Van Leer, B, "*Flux Vector Splitting for Euler Equations*", Lecture Notes in Physics, Vol. 170,p507.
- [15] Roe, Philip. L, B, "*Approximate Riemann Solvers, Parameter Vectors and Difference Schemes*", Journal of Computational Physics, Vol. 18, p337.

-
- [16] GAMM, "*Workshop on Numerical Solutions of Compressible Euler Flows*", June, 1986.
 - [17] AGARD AR 211, "*Test Cases for inviscid flow field methods*", Report of Fluid Dynamic Panel Working Group 07.
 - [18] Balakrishnan, N, "*Novel Schemes based on Wave-Particle Splitting for Compressible Flows*", Phd. Thesis of IISc-Bangalore (1995).
 - [19] Liepmann, H.W and Roshko, A, "*Elements of Gas Dynamics*", Wiley, 1957.
 - [20] Lerat, A, Sides, J, "*Efficient Solution of the steady Euler Equations with a centered implicit method*", Numerical Methods for Fluid Dynamics, ed. K.W. Morten et M.J. Baines, Clarendon Press-Oxford, pp.65-86,1988.